

Effect of Mn Doping on Electrical and Optical Behavior of Chemically Synthesized ZnTe Thin Film

Ujjwal Prasad ^a, Pushp Raj Harsh ^a, S.R. Kumar ^b, Kamal Prasad ^{a,*}

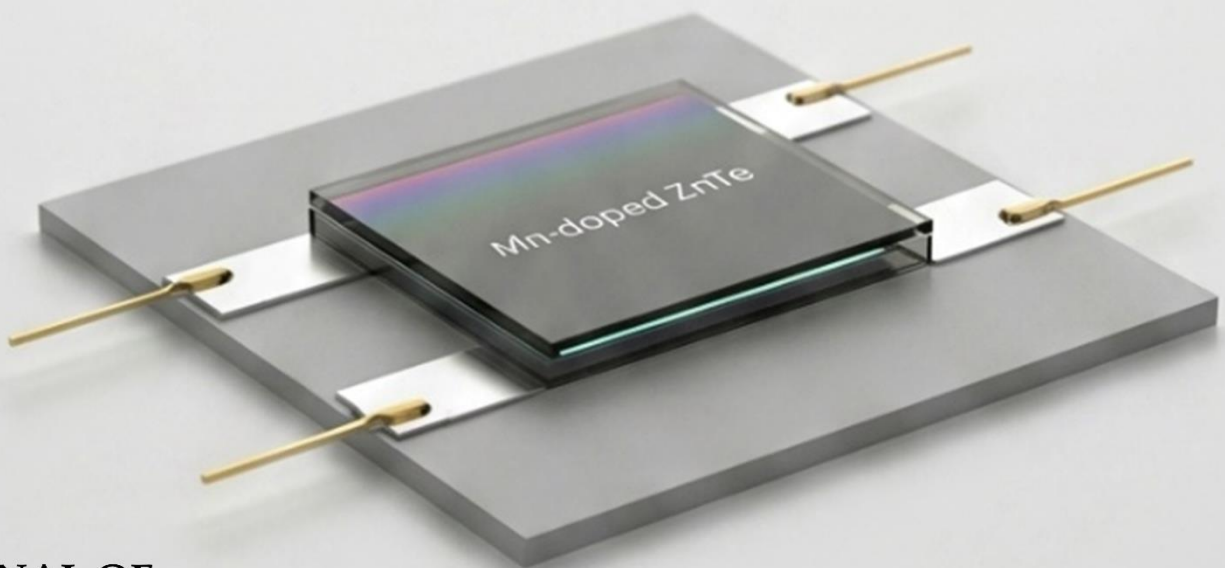
^a University Department of Physics, T.M. Bhagalpur University, Bhagalpur - 812007, India

^b Department of Applied Science and Humanities, NIAMT, Hatia, Ranchi - 834003, India

Editor's note: Zinc Telluride (ZnTe) is a II-VI semiconductor with a 2.26 eV band gap, ideal for optoelectronic devices like LEDs, solar cells, and laser diodes. Prasad et al. investigated the effects of manganese (Mn) doping on the properties of ZnTe thin films for optoelectronic applications. ZnTe and Mn-doped ZnTe films were deposited on FTO via chemical bath deposition. Structural analysis was conducted using X-ray diffraction (XRD), while optical properties were assessed through UV-Visible spectroscopy, and electrical behavior was evaluated with current-voltage measurements. Their results demonstrate that Mn doping enhances the properties of ZnTe thin films for use in photodetectors and photovoltaics.

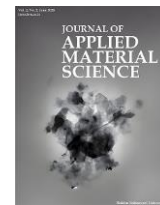
doi: 10.22034/jams.2026.260203

How to cite: U. Prasad et al., *Journal of Applied Material Science*, **2026**, 2, 260203.



JOURNAL OF
**APPLIED
MATERIAL
SCIENCE**

jams.hsu.ac.ir



Original Research

Effect of Mn Doping on Electrical and Optical Behavior of Chemically Synthesized ZnTe Thin Film

Ujjwal Prasad ^a, Pushp Raj Harsh ^a, S.R. Kumar ^b, Kamal Prasad ^{a,*}

^a University Department of Physics, T.M. Bhagalpur University, Bhagalpur - 812007, India

^b Department of Applied Science and Humanities, NIAMT, Hatia, Ranchi - 834003, India

Abstract

In this work, the structural, optical, and electrical properties of pure ZnTe and Mn-doped ZnTe thin films were examined to understand the effect of manganese (Mn) incorporation on the fundamental behavior of the material. ZnTe, a II-VI compound semiconductor, has gained significant attention due to its direct band gap, high optical absorption coefficient, and suitability for various optoelectronic applications. Introducing transition metal dopants such as Mn into the ZnTe lattice is a well-established strategy to modify and improve its optical properties, thereby enhancing its functional performance. The ZnTe and Mn-doped ZnTe thin films were deposited on FTO using the chemical bath deposition (CBD) technique. This method was chosen because of its simplicity, cost-effectiveness, and ability to produce uniform, well-adhered films over large areas. Structural characterization was carried out using X-ray diffraction (XRD) to investigate phase purity, crystallinity, preferred orientation, and possible lattice distortions resulting from Mn doping. Optical studies were performed using UV-Visible spectroscopy to analyze absorption characteristics and estimate the optical band gap, which provides insight into changes in the electronic structure due to Mn incorporation. Electrical behavior was evaluated using current-voltage (I-V) measurements to understand charge transport mechanisms, variations in conductivity, and the role of Mn in carrier movement. Overall, the combined structural, optical, and electrical investigations provide a clear picture of the influence of Mn doping on ZnTe thin films, demonstrating their promising potential for optoelectronic devices such as photodetectors and photovoltaic applications.

Keywords: Thin Film; ZnTe; XRD; Band Gap; I-V Characteristics; Optoelectronics; Photodetectors.

1. Introduction

Zinc Telluride (ZnTe) is a II-VI group binary compound semiconductor that has garnered interest in

recent years due to its favorable optical and electrical characteristics. One of the important features of ZnTe is its direct band gap of about 2.26 eV at room temperature, which lies in the visible region of the electromagnetic

* Corresponding author.

Email address: prasad_k@tmbuniv.ac.in (K. Prasad)

Received 30 January 2026

Revised 19 April 2026

Accepted 23 April 2026

Available online 17 May 2026

spectrum. This makes ZnTe highly suitable for applications wherever efficient light absorption or emission is required. Structurally, ZnTe typically crystallizes in the zinc-blende (cubic) phase, which is stable and well-suited for thin-film growth. These inherent properties make ZnTe a promising material for a wide range of optoelectronic devices, including light-emitting diodes, laser diodes, solar cells, and photodetectors.

A key advantage of ZnTe is its high absorption coefficient in the visible region. This allows the material to absorb a significant amount of incident light even when deposited as a thin film, which is particularly beneficial for photovoltaic and photodetector applications. Moreover, efficient light harvesting is essential for enhancing device performance, a requirement that ZnTe fulfills effectively. In addition, ZnTe exhibits excellent compatibility with other II-VI and III-V semiconductors, facilitating its integration into heterostructures and multilayer device architectures. Such compatibility enables band structure engineering and improved charge transport, which are essential for high-performance optoelectronic and photovoltaic systems [1]. However, despite all these, ZnTe also faces certain limitations that restrict its broader application.

One of the main challenges associated with ZnTe is its intrinsic p-type conductivity, which is largely attributed to native defects such as zinc vacancies. While p-type behavior is useful in some device structures, it becomes a limitation in applications that require n-type conductivity or balanced charge transport. Moreover, controlling the electrical properties of ZnTe remains challenging, as intrinsic defects can influence carrier concentration, mobility, and recombination processes, ultimately affecting device efficiency. To address these issues and optimize material performance, doping has been extensively investigated as an effective approach. In particular, transition metal dopants have attracted considerable attention owing to their capability to tailor both the electrical and optical properties of ZnTe [2].

Among various dopants, manganese (Mn) has emerged as a promising candidate for tailoring the properties of ZnTe. Mn incorporation enables modulation of the band structure, defect states, and charge transport behavior, thereby enhancing the material's suitability for device applications. The introduction of Mn ions into the ZnTe lattice can lead to slight structural modifications due to differences in ionic

size between Mn and Zn. These changes can affect crystallinity, grain growth, and defect distribution, all of which play an important role in determining the optical and electrical performance of the materials [3]. Use of Mn as a dopant may change its absorption edge and band gap, offering the possibility of tuning the optical response of ZnTe for specific applications.

Electrically, Mn doping can modify carrier concentration and mobility by introducing additional energy levels within the band gap, which influence charge transport and recombination processes [4]. Overall, ZnTe remains a highly attractive semiconductor material for optoelectronic and photovoltaic applications due to its direct band gap, strong optical absorption, and structural compatibility with other semiconductors. The controlled doping of ZnTe with manganese offers an effective pathway to overcome its intrinsic limitations and to tailor its properties for enhanced device performance. Continued investigation of Mn-doped ZnTe thin films is therefore crucial for the development of efficient and reliable next-generation optoelectronic devices [5].

2. Experimental

2.1. Materials

Analytical-grade chemicals: Tellurium dioxide, Zinc Acetate, Manganese Acetate, Ethylene Glycol, Sodium Hydroxide, Sodium Borohydride, and FTO-coated glass slide were procured from Sigma Aldrich.

2.2. Sample preparations

ZnTe and Mn-doped ZnTe thin films were prepared using the chemical bath deposition (CBD) technique. Tellurium dioxide (TeO_2) was employed as the source of Te^{2+} ions, while zinc acetate was used as the Zn^{2+} precursor. Ethylene glycol was selected as the solvent due to its high boiling point and its ability to regulate the controlled release of metal ions, which is essential for uniform film growth. Initially, 20 ml of ethylene glycol was heated to 140–150°C and mixed with 0.1 M zinc acetate under continuous magnetic stirring to obtain Solution A.

In a separate container, 0.1 M tellurium dioxide was dissolved in 20 ml of ethylene glycol. The solution was gently heated and continuously stirred, and sodium hydroxide was added dropwise until a clear and

transparent solution formed, indicating the formation of a stable tellurium complex. This solution was designated as Solution B. Subsequently, Solutions A and B were slowly combined under constant stirring to ensure homogeneous mixing and to avoid premature precipitation. After thorough mixing, 40 mg of sodium borohydride (NaBH_4) was introduced to the reaction bath, where it acted as a reducing agent to facilitate the formation of ZnTe.

For the preparation of Mn-doped ZnTe thin films, 0.001 M manganese acetate was added to Solution A before the addition of the tellurium precursor. Cleaned fluorine-doped tin oxide (FTO) substrates were vertically immersed in the reaction bath to promote uniform deposition and to minimize particulate settling on the film surface.

The chemical bath deposition process was carried out at a constant temperature of 150°C for 90 minutes. To maintain an alkaline reaction environment favorable for film formation, a few drops of ammonia solution were added to the bath periodically to adjust the pH to ~ 9 . After completion of the deposition process, the substrates were carefully removed from the bath, thoroughly rinsed with deionized water to remove loosely adhered particles and residual reactants, and then allowed to dry at room temperature.

2.2. Measurements

The structural properties of the deposited ZnTe and Mn-doped ZnTe thin films were subsequently characterized using X-ray diffraction (XRD) with $\text{CuK}\alpha$ radiation ($\lambda = 1.5406 \text{ \AA}$). The diffraction patterns were recorded over a 2θ range of 20° – 70° using a Rigaku Mini Flex 600 diffractometer to analyze phase composition, crystallinity, and the influence of Mn doping on the crystal structure. The optical properties of the films were studied using a JASCO V-770 Uv-Vis-NIR spectrophotometer. SEM images were obtained using a JEOL JSM-6360A at an operating voltage of 20 kV. Electrical measurements were performed at room temperature using a two-probe setup, using a Biologic potentiostat equipped with a booster to measure current in picoamperes.

3. Results and discussion

3.1. X-Ray diffraction

Figure 1 shows the XRD patterns of the undoped and Mn-doped ZnTe thin films deposited by the chemical bath deposition method. The presence of clear and well-defined diffraction peaks confirms that both films are polycrystalline in nature. Diffraction peaks are observed at 2θ values of 25.42° , 29.60° , 42.50° , 49.40° , and 66.50° ,

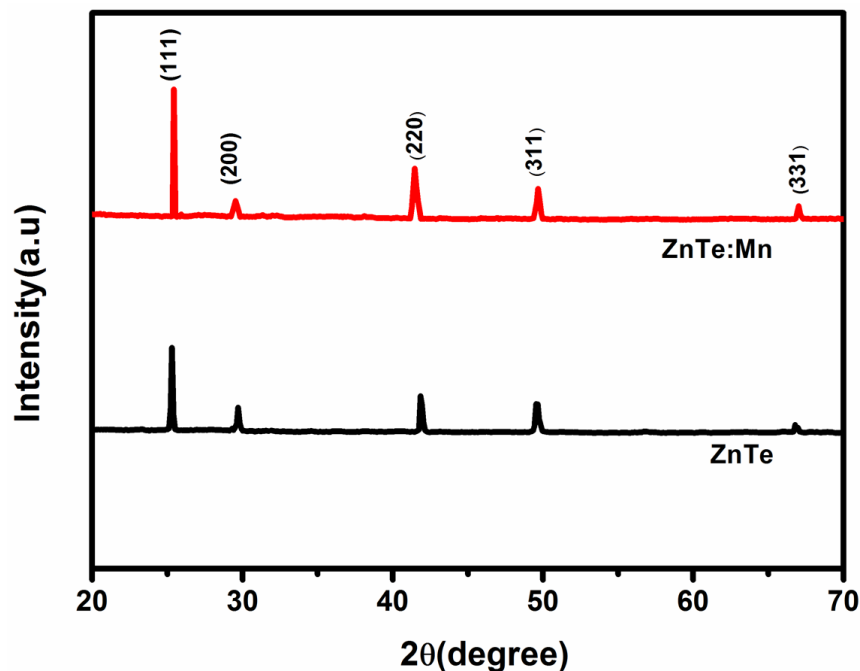


Figure 1. XRD patterns of ZnTe and Mn-doped ZnTe.

Table 1. Structural Parameters of ZnTe and Mn-doped ZnTe

Sample	2θ (°)	FWHM (°)	Crystallite Size (nm)	d spacing (nm)	Lattice constant 'a' (nm)	Microstrain
ZnTe	25.42	0.229	38	0.35024	0.60664	0.0044338
Mn-doped ZnTe	25.04	0.267	29	0.35575	0.61617	0.0052549

which can be indexed to the (111), (200), (220), (311), and (331) planes of cubic zinc-blende ZnTe, respectively. These peaks match well with the standard JCPDS data (Card No. 15-0746) [2, 6], confirming the formation of ZnTe with a cubic crystal structure. No additional peaks corresponding to secondary phases such as elemental Zn, Te, or manganese-related compounds are detected in the diffraction patterns. This indicates that the deposited films possess good phase purity and that the incorporation of Mn does not lead to the formation of unwanted impurity phases.

Notably, the Mn-doped ZnTe films exhibit the same set of diffraction peaks as the undoped ZnTe films, suggesting that Mn ions are successfully incorporated into the ZnTe lattice without altering its fundamental crystal structure. A closer comparison of the diffraction patterns reveals a slight shift of the peaks toward lower 2θ values after Mn doping. This shift suggests a small expansion of the lattice, which can be attributed to the substitution of Zn²⁺ ions by Mn²⁺ ions within the ZnTe lattice. Since Mn²⁺ ions have a slightly larger ionic radius than Zn²⁺ ions, their incorporation results in increased interplanar spacing, leading to the observed peak displacement. Such behavior further supports the successful substitutional incorporation of Mn into the ZnTe structure.

The average crystallite size of the undoped and Mn-doped ZnTe thin films was estimated using the Scherrer equation based on the XRD peak broadening. The calculated crystallite size values are listed in Table 1 and provide insight into the influence of Mn doping on the microstructural properties of ZnTe thin films. The Scherrer formula is given by [7]:

$$D = 0.9\lambda/\beta\cos\theta \quad (1)$$

For cubic systems, the lattice constant 'a' can be calculated using [8]:

$$a = d\sqrt{h^2 + k^2 + l^2} \quad (2)$$

where d is obtained from Bragg's law: $n\lambda = 2d\sin\theta$. The calculated 'd' value is shown in Table 1, and the calculated lattice parameter for cubic ZnTe is 0.60664 nm

and increased to 0.61617 nm after Mn doping. The increase in the lattice parameter is attributed to the substitutional incorporation of Mn²⁺ ions into Zn²⁺ lattice sites, resulting in modified bond lengths and lattice expansion. The observed increase confirms successful Mn incorporation into the ZnTe crystal structure while maintaining the cubic zinc-blende phase.

The microstrain of ZnTe and Mn-doped ZnTe thin films was evaluated using the equation:

$$\varepsilon = \frac{\beta}{4\tan\theta} \quad (3)$$

The microstrain of ZnTe thin films was found to be 0.0044338, which increased to 0.0052549 after Mn doping. The enhancement in microstrain is attributed to the substitutional incorporation of Mn ions into Zn lattice sites, leading to lattice distortion, increased defect density, and internal stress within the crystal structure. The observed increase in strain confirms successful Mn incorporation and structural modification of the ZnTe lattice.

3.2. Scanning Electron Microscopy

Figure 2 shows the cross-sectional SEM images of ZnTe and Mn-doped ZnTe. The cross-sectional SEM image of the ZnTe thin film reveals a continuous and compact layer uniformly deposited over the substrate surface. The film exhibits a well-defined interface between the substrate and the ZnTe layer, indicating good adhesion and controlled nucleation during chemical bath deposition. The ZnTe layer appears dense and homogeneous, free from major cracks or voids, composed of closely packed columnar grains extending along the growth direction.

The columnar morphology indicates that film growth occurs through an initial island nucleation process, followed by coalescence, which is characteristic of chemically deposited II-VI semiconductor films. The uniform thickness observed across the cross-section indicates stable growth kinetics and consistent ion supply during deposition. The cross-sectional SEM image of Mn-doped ZnTe shows noticeable

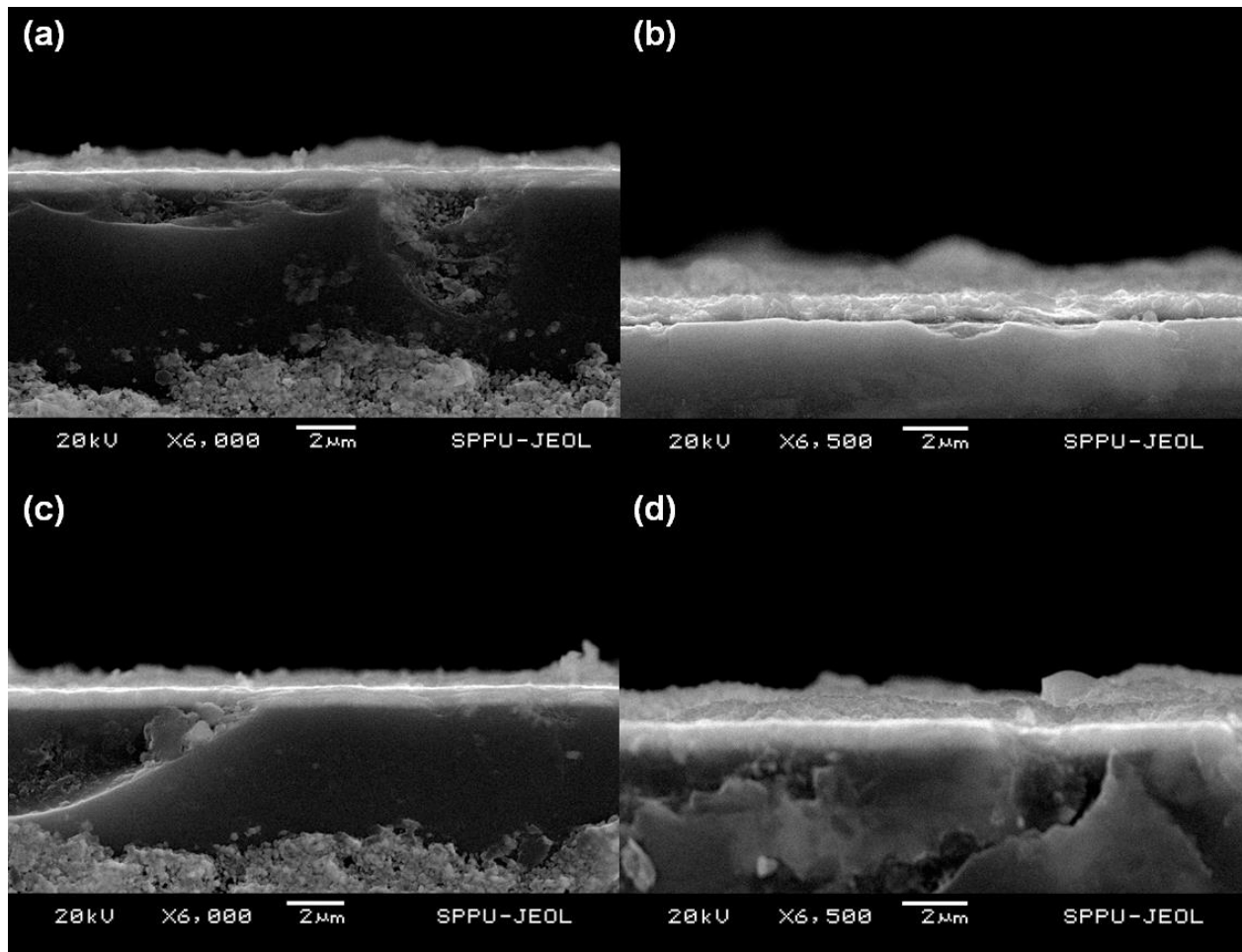


Figure 2. Cross-sectional SEM images of (a)-(b) ZnTe and (c)-(d) Mn-doped ZnTe.

modifications in microstructure compared to pure ZnTe. The film maintains a continuous layered structure; however, the internal morphology becomes comparatively more textured and compact. Slightly increased film thickness, enhanced grain packing density, reduced intergranular voids, and more pronounced columnar growth features are the key observations.

The incorporation of Mn ions alters nucleation and growth dynamics, leading to increased lattice distortion and modified grain evolution. Mn atoms act as additional nucleation centers, promoting finer grain formation and improved film densification. These morphological improvements facilitate efficient carrier transport across the film thickness, which correlates well with the observed enhancement in electrical performance [4, 9].

3.3. Optical band gap

The optical band gap is a key parameter of any semiconductor, as it determines how the material interacts with light and directly influences its performance in optoelectronic devices. In this study, the optical band gap of undoped and Mn-doped ZnTe thin films was evaluated using a UV-Visible spectrophotometer.

This technique provides valuable information about the light-absorption behavior of the films over a wide spectral range and is commonly employed for band gap estimation in thin film semiconductors. The absorbance data obtained from the UV-Visible measurements were used to calculate the absorption coefficient, which reflects the probability of electronic transitions between the valence and conduction bands.

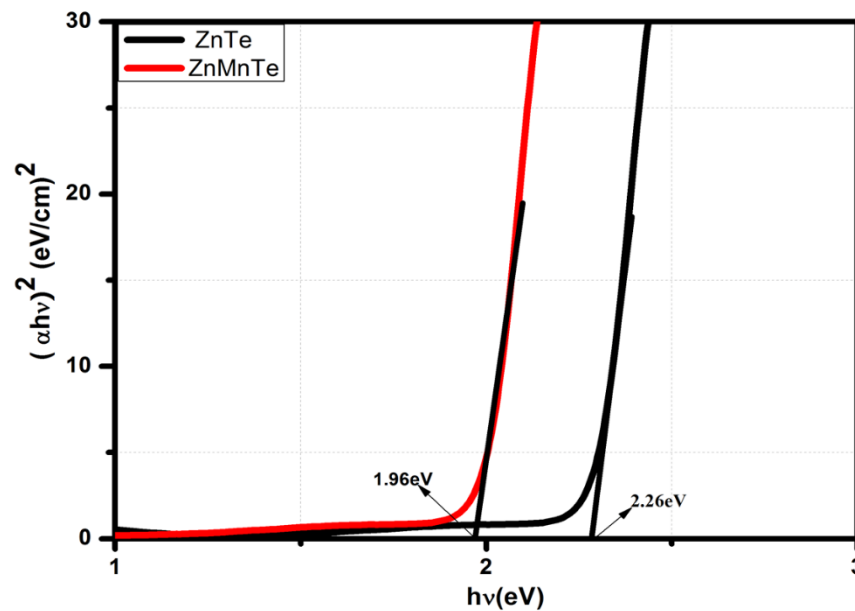


Figure 3. Tauc plot of ZnTe and Mn-doped ZnTe.

The Tauc method was applied to determine the band gap. Since ZnTe is a direct band gap semiconductor, Tauc plots were constructed by plotting $(\alpha h\nu)^2$ versus $h\nu$ as shown in Figure 3. The optical band gap was estimated by extrapolating the linear portion of the plot in the higher energy region to the photon energy axis. For ZnTe thin film, the Tauc plot exhibits a clear and well-defined linear region, indicating allowed direct electronic transitions. After extrapolation, the optical band gap value is 2.26 eV [10]. This value closely matches the reported band gap of bulk ZnTe, suggesting that the deposited film possesses good optical quality and that the deposition process does not introduce significant defects that would strongly affect the band structure.

In the case of Mn-doped ZnTe thin films, a noticeable change in the optical behavior is observed. Although the Tauc plot for the doped film still shows a linear region, confirming that the material maintains its direct band gap nature, the extrapolated band gap value is reduced to about 1.96 eV. This reduction in band gap indicates that the incorporation of Mn has a significant influence on the electronic structure of ZnTe. The band gap narrowing can be attributed to the introduction of impurity-related energy levels within the band gap, which arise due to the presence of Mn ions in the ZnTe lattice.

Mn ions introduce localized d-electron states inside the ZnTe band structure. These states create intermediate energy levels between the valence and conduction bands, which reduce the effective transition energy and narrow the optical band gap. Additionally, increased lattice strain and defect density contribute to band tailing effects, resulting in band gap narrowing. Similar behavior has been reported for the transition metal ions, which introduce localized electronic states inside the band structure [11]. The observed band gap value demonstrates that Mn doping is an effective approach for controlling the optical properties of ZnTe thin films, making them more suitable for applications such as photodetectors and photovoltaic devices, where enhanced absorption in the visible region is desirable [4].

3.4. Electrical study

Understanding the electrical behavior of ZnTe and Mn-doped ZnTe thin films is crucial for their application in photovoltaic cells, photodetectors, and other optoelectronic devices. Figure 4 shows the I-V characteristics of ZnTe and Mn-doped ZnTe (ZnMnTe) thin films deposited on fluorine-doped tin oxide (FTO) substrates using the chemical bath deposition technique. Here, the FTO layer acted as the transparent conducting front contact, while a silver (Ag) back contact was deposited by vacuum evaporation to ensure good

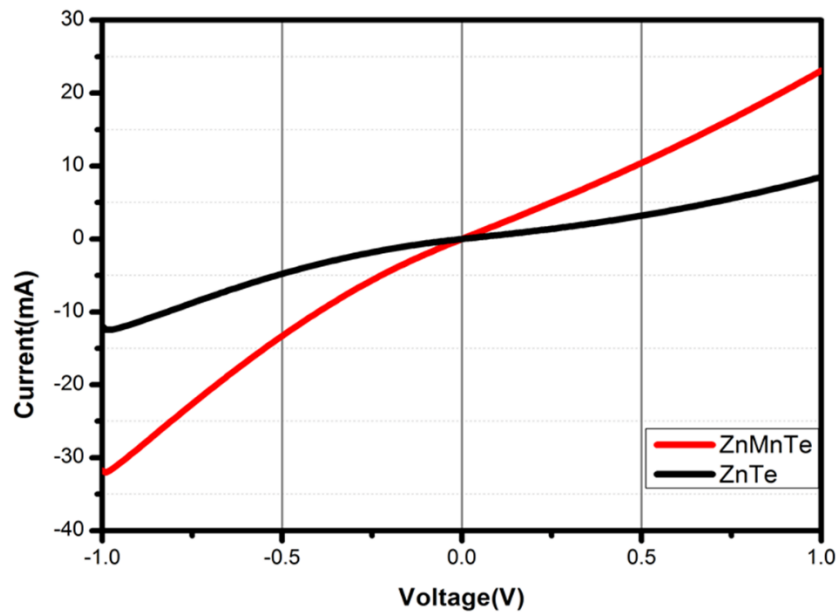


Figure 4. I-V curves of ZnTe and Mn-doped ZnTe.

electrical contact. This formed a metal–semiconductor junction suitable for evaluating rectifying behavior under forward and reverse-bias conditions. The undoped ZnTe thin film exhibits a clear diode-like behavior. In the forward-bias region, the current increases exponentially with applied voltage, indicating that charge transport is dominated by thermionic

emission across the potential barrier at the metal–semiconductor interface.

In the reverse-bias region, the current remains relatively low and nearly constant, confirming the blocking nature of the junction. This rectifying behavior suggests the formation of a Schottky-type contact between the ZnTe film and the metal electrode. Key

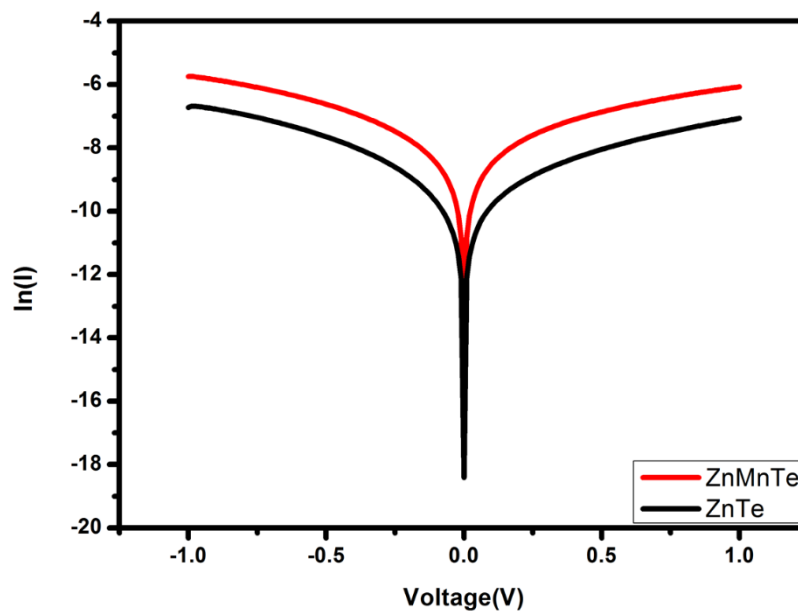


Figure 5. $\ln(I)$ vs. V curves of ZnTe and Mn-doped ZnTe.

parameters like ideality factor (η) and the Schottky barrier height (ϕ) were calculated from the forward bias region of the I-V curves using the equations [12]:

$$\phi = \frac{kT}{q} \ln \left(\frac{AA^*T^2}{I_s} \right) \quad (4)$$

$$\eta = \left(\frac{q}{kT} \right) \left(\frac{dV}{\ln I} \right) \quad (5)$$

Here, V is the applied voltage, η is the ideality factor, ϕ is the potential barrier height, A is the contact area, and I_s is the saturation current. To get η and ϕ , the linear part of the $\ln(I)$ vs. voltage (V) curves in Figure 5 was sloped and intercepted [13].

The calculated value of potential barrier and ideality for the pure and Mn-doped ZnTe thin films are 0.86 V, 1.47, and 0.55 V, 1.27, respectively. The ideality factor provides information about the deviation of the diode behavior from ideal conditions, while the barrier height represents the energy barrier that charge carriers must overcome to contribute to current flow. For the ZnTe thin film, the ideality factor was found to be greater than 1.47, indicating the presence of additional transport mechanisms such as recombination, interface states, or series resistance effects.

Upon Mn doping, a noticeable enhancement in the electrical response is observed. The Mn-doped ZnTe thin film exhibits a higher forward current at the same applied voltage compared to the undoped film, reflecting improved conductivity. This enhancement can be attributed to the incorporation of Mn ions into the ZnTe lattice, which increases the carrier concentration and modifies the band structure. The ideality factor for the Mn-doped film is reduced compared to the undoped sample, suggesting improved junction quality and reduced recombination losses at the interface [11]. Furthermore, Mn incorporation lowers the effective barrier height, promoting more efficient charge-carrier transport across the interface.

While undoped ZnTe primarily follows thermionic emission transport, Mn incorporation increases carrier concentration and narrows the depletion region, enabling thermionic-field emission and tunneling-assisted transport. Also, Mn reduces interface defect density, lowering recombination losses and improving the ideality factor. These combined effects facilitate more efficient charge transport, resulting in enhanced diode performance and superior electrical characteristics of Mn-doped ZnTe thin films.

In short, the extracted ideality factor and barrier height values demonstrate that Mn doping significantly improves the electrical characteristics of ZnTe thin films. The enhanced conductivity, lower barrier height, and improved junction quality highlight the potential of Mn-doped ZnTe for efficient optoelectronic device applications, particularly in photodetectors and photovoltaic systems [14].

4. Conclusions

The shift in diffraction peaks and decrease in crystallite size with Mn doping indicate the successful substitution of Mn^{2+} ions into the ZnTe lattice. The V-I characteristics of ZnTe and Mn-doped ZnTe thin films reveal significant differences in their electrical behavior, particularly in forward and reverse-bias regions. Also, Mn doping enhances electrical performance by increasing carrier concentration, reducing series resistance, and passivating defect states, resulting in higher forward current and lower reverse-bias leakage. Further, Mn doping enhances the optical properties by reducing the energy band gap, as confirmed by UV-Visible spectroscopy. The enhanced conductivity, lower barrier height, and improved junction quality highlight the potential of Mn-doped ZnTe for efficient optoelectronic device applications, particularly in photodetectors and photovoltaic systems.

Conflict of Interest

The authors declare no conflict of interest.

References

1. K.L. Chopra, et al., *Chemical Solution Deposition of Inorganic Films*, in *Physics of Thin Films*. **1982**, Elsevier. p. 167.
2. T. Wojtowicz, et al. MBE Growth and Properties of ZnTe- and CdTe-Based Nanowires. *Journal of the Korean Physical Society*, **2008**, 53, 3055.
3. Y.L. Cao, et al. Single-crystalline ZnTe nanowires for application as high-performance Green/Ultraviolet photodetector. *Optics Express*, **2011**, 19, 6100.
4. V.V. Brus, et al. Specific features of the optical and electrical properties of polycrystalline CdTe films grown by the thermal evaporation method. *Physics of the Solid State*, **2014**, 56, 1947.

5. K. Singh, et al. Determination of Structural Elements of Hydrothermally Synthesized CeO₂ Nanoparticles by Monshi, Williamson-Hall, Halder-Wagner, and Size-Strain Plot Methods, and Effect of Annealing Temperature. *Macromolecular Symposia*, **2024**, 413, 2400104.
6. S. Tyagi, et al. MBE-grown ZnTe epitaxial layer based broadband photodetector with high response and excellent switching characteristics. *Semiconductor Science and Technology*, **2024**, 39, 095005.
7. S.A. Disha, et al. Calculation of crystallite sizes of pure and metals doped hydroxyapatite engaging Scherrer method, Halder-Wagner method, Williamson-Hall model, and size-strain plot. *Results in Materials*, **2024**, 21, 100496.
8. Z.M. Nassar, M.H. Yükselici, and A.A. Bozkurt. Structural and optical properties of CdTe thin film: A detailed investigation using optical absorption, XRD, and Raman spectroscopies. *physica status solidi (b)*, **2016**, 253, 1104.
9. M. Imamura, et al. Magneto-optical properties of wider gap semiconductors ZnMnTe and ZnMnSe films prepared by MBE. *Journal of Electronic Science and Technology*, **2020**, 18, 100056.
10. S. Adachi, *Zinc Telluride (ZnTe)*, in *Optical Constants of Crystalline and Amorphous Semiconductors*. **1999**, Springer US. p. 473.
11. F. El Akkad and Y. Abdurraheem. Morphology, electrical, and optical properties of heavily doped ZnTe:Cu thin films. *Journal of Applied Physics*, **2013**, 114, 183501.
12. S.M. Sonawane, S. Chaure, and N.B. Chaure. Characterization of Sb₂Te₃ thin films prepared by electrochemical technique. *Journal of Physics and Chemistry of Solids*, **2023**, 172, 111095.
13. A. Ukarande, et al. Wet-electrochemical growth of CdTe layers for photovoltaic applications. *Journal of Materials Science: Materials in Electronics*, **2022**, 33, 22456.
14. A. Jrad, et al. Effect of manganese concentration on physical properties of ZnS:Mn thin films prepared by chemical bath deposition. *Journal of Materials Science: Materials in Electronics*, **2016**, 28, 1463.

© 2026 Authors. The authors retain the copyright and full publishing rights. This article is licensed under a Creative Commons Attribution 4.0 BY International License. 